

Supplementary Appendix

This appendix has been provided by the authors to give readers additional information about their work.

Supplement to: Pedchenko V, Bondar O, Fogo AB, et al. Molecular architecture of the Goodpasture autoantigen in anti-GBM nephritis. N Engl J Med 2010;363:343-54.

Supplementary Appendix

This appendix has been provided by the authors to give readers additional information about their work.

Supplement to: Pedchenko V, Bondar O, Vanacore R, et al. Goodpasture Syndrome/Anti-GBM Glomerulonephritis: An Autoimmune Conformeropathy. N Engl J Med 2009

SUPPLEMENTARY APENDIX

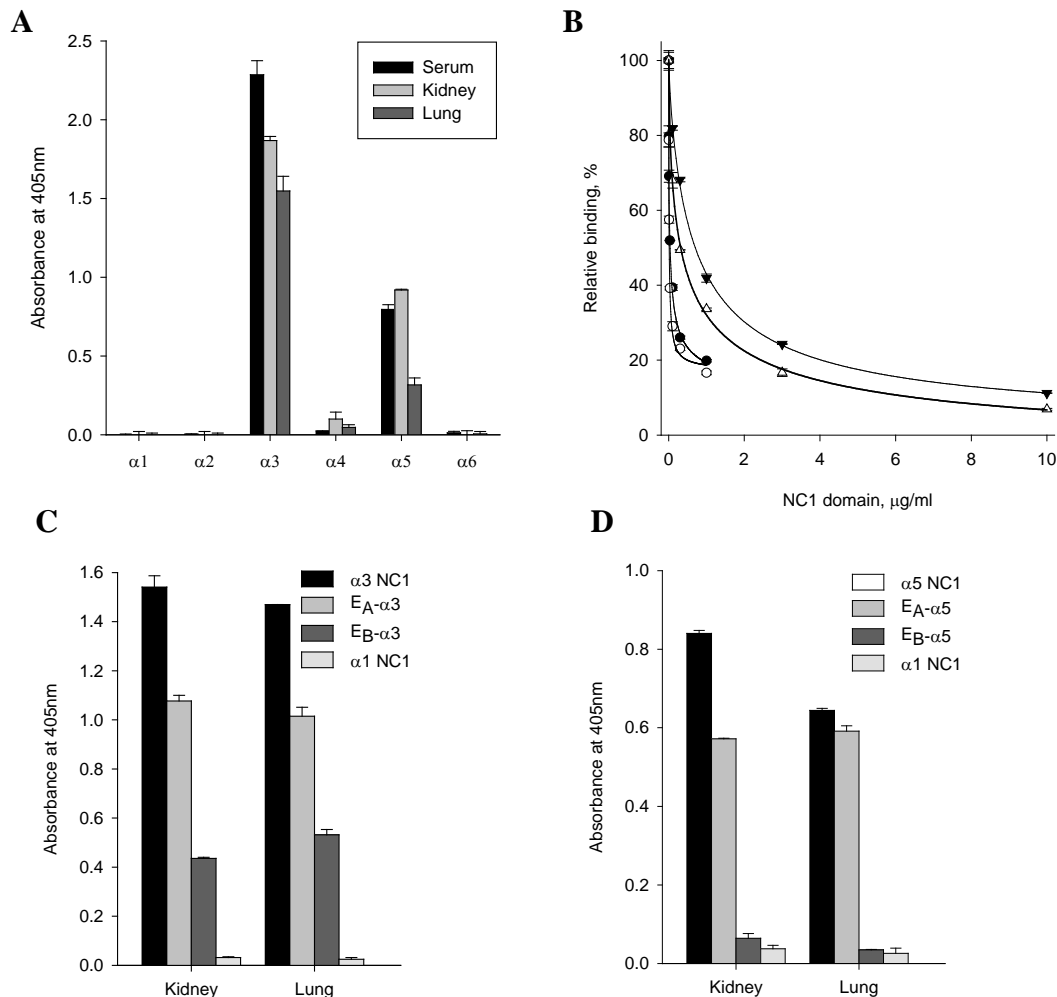
DETAILED METHODS

PROTEINS

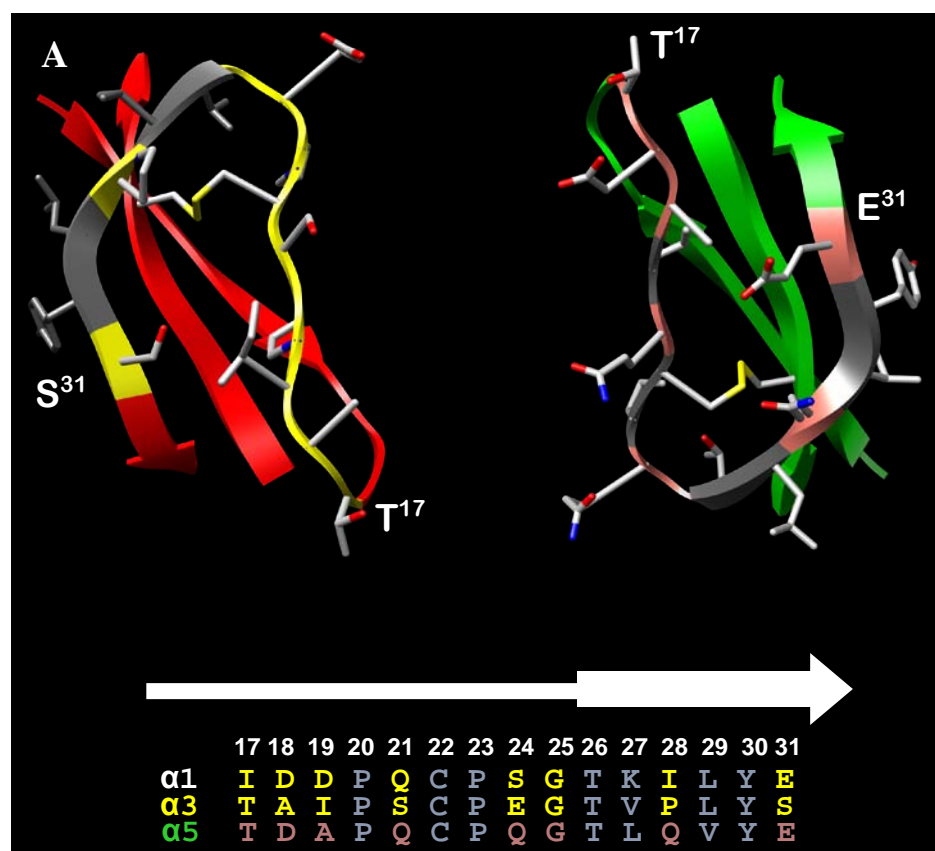
For the construction of $\alpha 5/\alpha 1$ chimeras corresponding to E_A and E_B epitopes of $\alpha 3NC1$ domain, we used three-stage PCR mutagenesis with pRc/ $\alpha 1$ vector as a template¹. At the first stage, 5' and 3' parts of $\alpha 1NC1$ were amplified using primer pairs which introduced partial substitutions within E_A and E_B regions. At the next stage substitutions were completed using overlapping primers, and $\alpha 1NC1$ complementary sequences were introduced at the 3' or 5' ends of PCR products. Resulting fragments were purified and used as megaprimers in a third PCR with the flanking primers to generate the cDNA for the entire coding region of the chimeras. After digestion with *NheI/SacII* final constructs were ligated into the pRc/CMV expression vector. Introduction of the desired mutations was verified by automated sequencing. Constructs were stably transfected into HEK 293 cells and chimeras were purified from the culture medium using anti-FLAG agarose.²

HOMOLOGY MODELING

The model of $\alpha 345NC1$ hexamer was constructed by homology modeling and molecular dynamics simulation based on the crystal structure of the $\alpha 112NC1$ hexamer³ (PDB accession code: 1M3D) as described.⁴ The final model was analyzed using Chimera,⁵ and accessible surface area of residues was determined using AREAIMOL (CCP4 suite, v.6.0).⁶



Supplementary Figure 1. Comparison of circulating, kidney- and lung-bound autoantibodies from one patient with Goodpasture's disease. Panel **A** shows similar NC1 monomers specificity of serum, lung and kidney eluates. Panel **B** shows that circulating and kidney-bound GP autoantibodies have similar affinities for their antigens. Binding of purified $\alpha 3\text{NC1}$ (●), $\alpha 5\text{NC1}$ (▼) and kidney-bound autoantibodies (○, Δ) from the same patient to $\alpha 3\text{NC1}$ or $\alpha 5\text{NC1}$ monomers was inhibited to the similar extent upon preincubation with corresponding antigens. Data are means \pm SE of representative experiment. Panels **C** and **D** shows that kidney- and lung-bound autoantibodies from the same GP patient have similar epitope specificity as measured by indirect ELISA with E_A and E_B chimeras of $\alpha 3\text{NC1}$ and $\alpha 5\text{NC1}$ monomers. Bars indicate means \pm SD of three independent experiments.



Supplementary Figure 2. Topology of the E_A region in α3NC1 and α5NC1 subunits of α345 NC1 hexamer and surface analysis of exposed/buried residues. E_A region in α3NC1 and α5NC1 are shown as ribbon diagrams (*top*); two residues in each region are shown for orientation. Each region is characterized by a loop-extended hairpin structure between two short β-strands, which forms anti-parallel β-sheet with remote β-strands from non-contiguous sequences of the same NC1 subunit (*red* and *green*), and a disulfide bond between conservative cysteine residues (Cys²²-Cys¹¹³, *yellow*) that stabilizes structural motif. A sequence alignment of the E_A regions of α1NC1, α3NC1, and α5NC1 is shown at the *bottom*. Buried residues are colored in *gray*; exposed residues are colored in *yellow* for the E_A-α3 and in *pink* for the E_A-α5, respectively. Wide white arrow above sequences depicts the location of β-sheets.

REFERENCES FOR SUPPLEMENTARY APPENDIX

1. Netzer KO, Leinonen A, Boutaud A, et al. The Goodpasture autoantigen. Mapping the major conformational epitope(s) of $\alpha 3(\text{IV})$ collagen to residues 17-31 and 127-141 of the NC1 domain. *J Biol Chem* 1999;274:11267-74.
2. Sado Y, Boutaud A, Kagawa M, Naito I, Ninomiya Y, Hudson BG. Induction of anti-GBM nephritis in rats by recombinant $\alpha 3(\text{IV})\text{NC1}$ and $\alpha 4(\text{IV})\text{NC1}$ of type IV collagen. *Kidney Int* 1998;53:664-71.
3. Sundaramoorthy M, Meiyappan M, Todd P, Hudson BG. Crystal structure of NC1 domains. Structural basis for type IV collagen assembly in basement membranes. *J Biol Chem* 2002;277:31142-53.
4. Vanacore RM, Ham AJ, Cartiailler JP, et al. A Role for Collagen IV Cross-links in Conferring Immune Privilege to the Goodpasture Autoantigen: STRUCTURAL BASIS FOR THE CRYPTICITY OF B CELL EPITOPES. *J Biol Chem* 2008;283:22737-48.
5. Pettersen EF, Goddard TD, Huang CC, et al. UCSF Chimera--a visualization system for exploratory research and analysis. *Journal of computational chemistry* 2004;25:1605-12.
6. The CCP4 suite: programs for protein crystallography. *Acta crystallographica* 1994;50:760-3.